ACS Photonics

Letter

pubs.acs.org/journal/apchd5

Near-Perfect Photon Tunneling by Hybridizing Graphene Plasmons and Hyperbolic Modes

Xianglei Liu,[†] Richard Z. Zhang,[†] and Zhuomin Zhang*

George W. Woodruff School of Mechanical Engineering, Georgia Institute of Technology, Atlanta, Georgia 30332, United States

ABSTRACT: Excitation of surface plasmon polaritons helps to increase the near-field heat flux by orders of magnitude beyond the limit governed by Stefan−Boltzmann law. However, the photon tunneling probability is rather low, except for modes satisfying the resonance condition of surface plasmon polaritons. Broadband hyperbolic metamaterials can broaden the frequency region for the enhancement of near-field heat transfer, but can hardly maintain a high tunneling probability for large wavevectors since no resonances are excited to overcome the inherent exponential decay. In this letter, perfect photon tunneling with near-unity probability across broad frequency and *k*-space region is demonstrated based on the hybridization of graphene plasmons and hyperbolic modes. As a result, the near-field heat transfer coefficient between doped-silicon-nanowire hyperbolic metamaterials can be further improved several fold when covered by a graphene sheet, approaching to a theoretical limit.

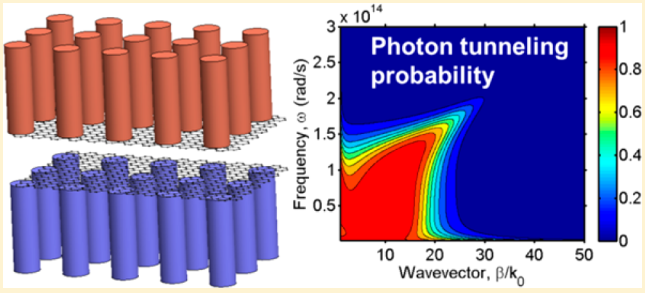

KEYWORDS: *graphene, hyperbolic metamaterials, near field, radiative heat transfer*

Radiative heat transfer between macroscopic bodies in the far field will achieve the maximum value if every photon emitted by one substance with any direction can be totally absorbed by the other body, indicating that the photon transmission probability is unity. These two substances are called blackbodies, and the radiative heat transfer between them is governed by the well-known Stefan−Boltzmann law, an upper limit for propagating modes.[1] Capturing incident photons with near-unity efficiency is also a desire in the near field due to the wide potential applications of near-field thermal radiation in local thermal management,[2] thermal imaging,[3,4] contactless thermal modulators,[5,6] and thermophotovoltaic (TPV) cells.[7,8]

Tunneling of evanescent modes enables the radiative heat flux to be several orders of magnitude higher than that between far-field blackbodies, especially when surface plasmon or phonon polaritons (SPPs) are excited.[1,9−11] Due to its unique characteristics, graphene can support surface plasmons with low loss and excellent tunability ranging from near-infrared to terahertz frequencies.[12] Graphene has been reported to tailor the near-field heat transfer[13−16] and improving the efficiency of TPV cells.[8,17] However, the near-unity photon tunneling probability occurs only in narrow wavevector or *k*-space range, where coupled SPPs are excited. Hyperbolic materials, featuring unbounded density of states, have been shown to enhance the photon tunneling probability.[18−22] However, since hyperbolic modes are resonance free, the tunneling probability unavoidably decays with increasing *k*. By combining graphene plasmons and hyperbolic modes, this work demonstrates photon tunneling with near-unity probability across a broad frequency range and large *k*-space.

The geometric arrangement of near-field thermal radiation between graphene-covered D-SiNW arrays is illustrated in Figure 1. Coating graphene on the top of silicon nanowires is a mature technology.[23] In the near field, the effective medium theory (EMT) is applicable if the nanowire period *P* is shorter than the smallest contributing wavelength, corresponding to the

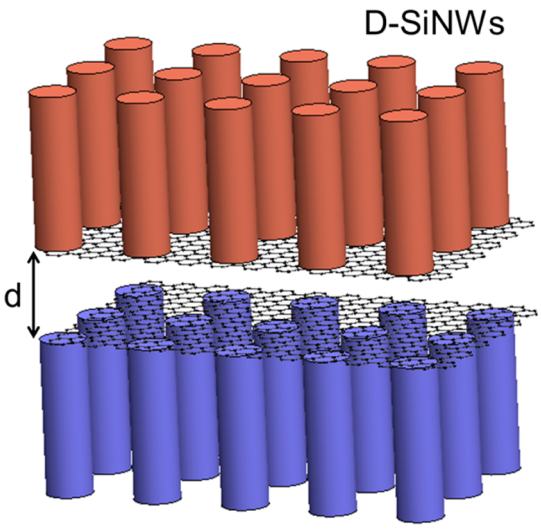

Figure 1. Schematic of near-field radiative heat transfer between graphene-covered semi-infinite doped silicon nanowires separated by a vacuum gap of distance *d*.

Received: May 13, 2014
Published: August 15, 2014

   dx.doi.org/10.1021/ph5001633 | *ACS Photonics* 2014, 1, 785−789

cutoff wavevector. The cutoff wavevector for hyperbolic modes has been given based on a 90% criterion as $1.94/d$.[24] Thus, EMT is expected to be a reasonable approximation when $d > 0.31P$. Under this condition, the nanowire composites can be homogenized as an effective uniaxial medium whose optical axis is parallel to the wire. The dielectric functions for orthogonal directions can be expressed as[20]

$$\varepsilon_E = 1 - f + \varepsilon_{D\text{-}Si} f \tag{1}$$

$$\varepsilon_O = \frac{\varepsilon_{D\text{-}Si} + 1 + (\varepsilon_{D\text{-}Si} - 1)f}{\varepsilon_{D\text{-}Si} + 1 - (\varepsilon_{D\text{-}Si} - 1)f} \tag{2}$$

where f is the volume filling ratio of doped silicon, ε_O (ordinary) and ε_E (extraordinary) are the dielectric functions for electric field perpendicular and parallel to the optical axis, respectively. When ε_O and ε_E have different signs, a hyperbolic dispersion will be supported. The doping level is set to be 10^{20} cm^{-3}, at which D-SiNWs have been shown to support a broadband hyperbolic dispersion.[20] The dielectric function of heavily doped silicon can be described by a Drude model $\varepsilon_{D\text{-}Si}(\omega) = 11.7 - \omega_p^2/(\omega^2 + i\gamma\omega)$ with a plasma frequency $\omega_p = 1.08 \times 10^{15}$ rad/s and scattering rate $\gamma = 9.34 \times 10^{13}$ rad/s.[25] The optical conductivity of graphene $\sigma(\omega)$ depends on chemical potential μ, electron relaxation time τ, and temperature T. The expression of $\sigma(\omega)$ can be found in refs 8 and 26. For convenience, the relaxation time is fixed to be $\tau = 10^{-13}$ s considering electron−phonon and electron−defects scattering,[27] while μ is adjusted to maximize the performance.

The radiative heat transfer coefficient at $T = 300$ K for the two media shown in Figure 1 can be calculated from[28]

$$h = \frac{1}{4\pi^2}\int_0^\infty g(\omega, T)\mathrm{d}\omega \int_0^\infty \sum_{j=s,p} \xi_j(\omega, \beta)\beta \mathrm{d}\beta \tag{3}$$

where ω is the angular frequency, β is the lateral wavevector, j represents either s- or p-polarization, and $g(\omega,T) = (\partial/\partial T)$-$[(\hbar\omega)/(e^{\hbar\omega/k_B T} - 1)]$ with k_B being the Boltzmann constant and $\hbar$ being the reduced Planck constant. In eq 3, $\xi(\omega,\beta)$ is called the energy transmission coefficient whose upper limit is unity and can be expressed in the following[19]

$$\xi_j(\omega, \beta) = \begin{cases} \dfrac{(1 - |r_j|^2)^2}{|1 - r_j^2 e^{2ik_{z0}d}|^2}, & \beta < k_0, \text{ propagating mode} \\ \dfrac{4[\mathrm{Im}(r_j)]^2 e^{-2|k_{z0}|d}}{|1 - r_j^2 e^{2ik_{z0}d}|^2}, & \beta > k_0, \text{ evanescent mode} \end{cases} \tag{4}$$

where r_j is the Fresnel reflection coefficient for given polarization and it is assumed that the two media have identical optical properties, k_0 is the vacuum wavevector, and k_{z0} is the z-component wavevector in vacuum. When $\beta < k_0$, $\xi(\omega,\beta)$ equals the far-field transmittance;[1] when $\beta > k_0$, $\xi(\omega,\beta)$ becomes the photon tunneling probability. The Fresnel coefficients for a graphene-covered uniaxial material can be obtained by imposing boundary conditions such that the tangential electric field remains continuous across the interface, while surface current enabled by graphene leads to a discontinuity of the tangential magnetic field. It follows that[8]

$$r_s = \frac{k_{z0} - \sqrt{k_0^2\varepsilon_O - \beta^2} - \sigma\mu_0\omega}{k_{z0} + \sqrt{k_0^2\varepsilon_O - \beta^2} + \sigma\mu_0\omega} \tag{5}$$

$$r_p = \frac{\varepsilon_O k_{z0} - k_{zp} + \sigma k_{z0}k_{zp}/\omega\varepsilon_0}{\varepsilon_O k_{z0} + k_{zp} + \sigma k_{z0}k_{zp}/\omega\varepsilon_0} \tag{6}$$

where μ_0 is the vacuum permeability and $k_{zp} = (k_0^2\varepsilon_O - \beta^2\varepsilon_O/\varepsilon_E)^{1/2}$ is the z-component of the wavevector in the uniaxial medium for p-polarization. When σ is set as zero, eqs 5 and 6 recover to the reflection coefficients between vacuum and a uniaxial medium.[20] When both ε_O and ε_E are set to 1 in eqs 5 and 6, the reflection coefficients are for suspended graphene sheets.

The calculated heat transfer coefficient h between graphene-covered D-SiNWs with $d = 200$ nm, $f = 0.02$, and $\mu = 0.3$ eV is 614.7 W/m^2-K, which is 4.5× as large as that for D-SiNWs. In order to unveil the underlying mechanism for this enhancement, the photon tunneling probability for p-polarization is plotted in Figure 2 for D-SiNWs, suspended graphene, and

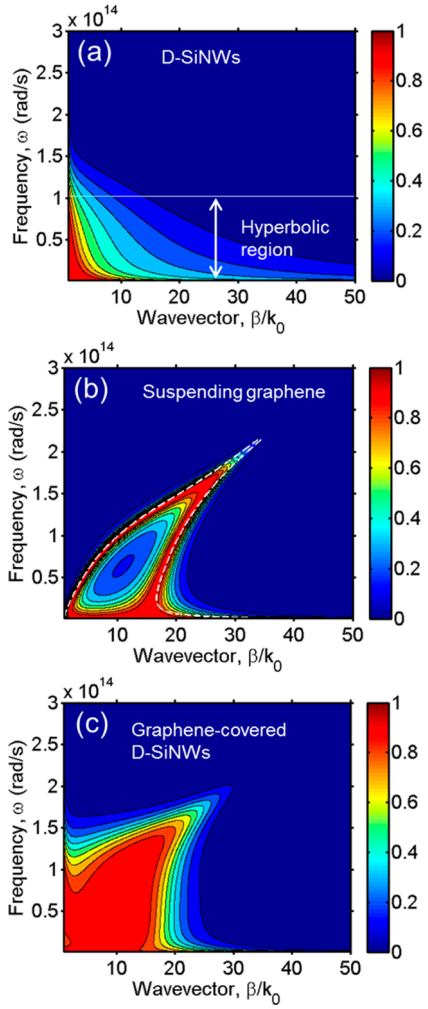

Figure 2. Photon tunneling probability for p-polarization at $d = 200$ nm and the value of $\xi_p(\omega,\beta)$ is indicated by the color contour for three different configurations. (a) Two D-SiNWs with $f = 0.02$ without graphene. (b) Suspended graphene with a chemical potential of 0.3 eV. The white lines delineate the two branches of coupled SPPs given by eqs 7 and 8. (c) Graphene-covered D-SiNWs.

dx.doi.org/10.1021/ph5001633 | ACS Photonics 2014, 1, 785−789

graphene covered nanowires for p-polarization evanescent modes. Note that the contributions to near-field radiative transfer from both the propagating and s-polarized evanescent waves are negligible compared to that of p-polarization evanescent waves capable of supporting hyperbolic or surface modes. As shown in Figure 2a by the color contour, the photon tunneling probability is much higher in the hyperbolic band than that in the nonhyperbolic region at frequencies exceeding 1.02×10^{14} rad/s. Due to the broadband hyperbolic modes, h for D-SiNWs achieves 135.3 W/m^2·K, which is 21× greater than the blackbody limit of $4\sigma_{SB}T^3$, where σ_{SB} is the Stefan–Boltzmann constant. Nevertheless, $\xi_p(\omega,\beta)$ inevitably decreases with increasing β due to the exponential decay factor of $e^{-2|k_{z0}|d}$ in the numerator of eq 4 since no resonance is excited.

Figure 2b gives ξ_p for suspended graphene sheets without substrates using $\mu = 0.3$ eV. There exist two distinct bands with large tunneling probability. These two bands, splitting at low β values and merging together at a large β, are associated with the coupled SPPs caused by the graphene. The dispersion relation can be obtained by zeroing the denominator of ξ_p and is given as[29]

$$1 + \frac{\sigma k_{z0}}{\omega\varepsilon_0} = \coth\left(\frac{ik_{z0}d}{2}\right), \quad \text{symmetric branch} \tag{7}$$

$$1 + \frac{\sigma k_{z0}}{\omega\varepsilon_0} = \tanh\left(\frac{ik_{z0}d}{2}\right), \quad \text{antisymmetric branch} \tag{8}$$

The low-frequency symmetric branch and the high-frequency antisymmetric branch are shown as the white lines in Figure 2b and match well with the peaks in ξ_p. Instead of decaying exponentially with β, the tunneling probability is almost unity when either eq 7 or eq 8 is satisfied. The diminishing denominator can compensate the decay factor $e^{-2|k_{z0}|d}$ in the numerator, enabling a large tunneling probability at large β values. The coupled SPPs have a dominant contribution to the near-field radiative heat transfer. As a result, the calculated heat transfer coefficient for two free-standing graphene sheets at d = 200 nm is as high as 453.7 W/m^2·K, even larger than that for D-SiNWs. However, the near-unity tunneling probability occurs in narrow β bands only.

When graphene covers the D-SiNWs for both the emitter and receiver, as shown in Figure 2c, ξ_p is very high across a broad frequency range up to 1.5×10^{14} rad/s and a large k-space up to $20k_0$. All the photons emitted in this regime will be absorbed, which is the blackbody behavior in the near field. As a result, the heat transfer coefficient of this hybrid structure could achieve 614.7 W/m^2·K, much larger than that for plain D-SiNWs or suspended graphene sheets alone.

The variation of ξ_p with β can be more clearly seen by comparing the three configurations at $\omega = 5 \times 10^{13}$ rad/s, which lies in the hyperbolic region, as illustrated in Figure 3. The tunneling probability of the resonance-free hyperbolic D-SiNWs decays quickly with increasing β; while that for the suspended graphene sheets has two resonance-like near-unity peaks. Interestingly, ξ_p for graphene-covered D-SiNWs can exceed 0.95 up to $\beta = 15k_0$. However, with further increasing β, the tunneling probability for graphene-covered D-SiNWs decreases rapidly and becomes lower than that between D-SiNWs for $\beta > 20k_0$. It can be seen from eq 6 that the terms containing σ are proportional to β^2, while the rest are proportional to β and thus become negligible at very large β. Specifically, when $\beta \gg c_0\varepsilon_0k_0/|\sigma|$, $r_p = 1$ with a zero imaginary

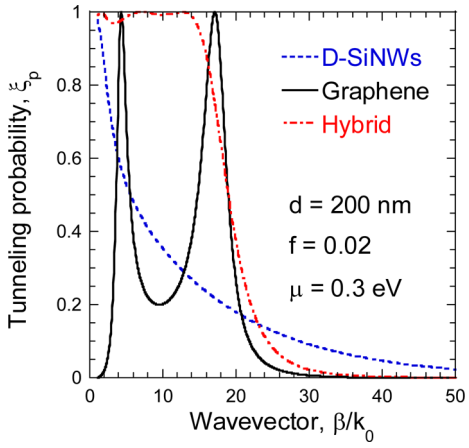

Figure 3. Photon tunneling probability at $\omega = 5 \times 10^{13}$ rad/s as a function of the lateral wavevector for the three configurations described in Figure 2

part. Subsequently, the photon tunneling probability becomes zero. Therefore, adding graphene suppresses phonon tunneling for very large β values, as can be seen from Figure 3. Nevertheless, the contribution by the perfect photon tunneling region dominates the near-field radiative transfer, resulting in a net enhancement.

Note that the graphene coverage does not always improve heat transfer.[14] For very small μ, coupling between graphene plasmons and hyperbolic modes becomes so weak that the improvement diminishes. Since σ generally increases with μ, more modes are adversely affected if μ is too high, leading to a deterioration of heat transfer performance. For a given filling ratio and specified gap distance, there exists an optimal chemical potential that allows near-perfect photon tunneling to be achieved in a broad frequency and wavevector ranges. The filling ratio can have a significant influence on the near-field radiative transfer as demonstrated previously without graphene coverage.[20] For very small f, the nanowire density is so dilute that the heat flux between graphene-covered nanowires approaches to that for suspended graphene. Too high a filling ratio makes both ε_O and ε_E negative such that no hyperbolic modes and hybridized perfect tunneling can occur. In the present study, f is chosen to be 0.02, which allows great enhancement of near-field radiation over a large distance range.

Figure 4a plots the heat transfer coefficient of D-SiNWs and graphene-covered nanowires at the optimal chemical potential given in Figure 4b, considering only p-polarized evanescent modes. The minimum d used here is 100 nm to ensure EMT is valid given that practical nanowire diameter cannot be infinitesimal. By optimizing the chemical potential, the inclusion of graphene can improve the near-field heat transfer between D-SiNWs. Heat transfer coefficient for graphene-covered D-SiNWs lies between that for D-SiNWs and the theoretical limit of hyperbolic materials given by[19]

$$h_{\text{limit}} = \frac{k_B^2 T \ln(2)}{12\hbar d^2} \tag{9}$$

as shown in Figure 4a. The ratio of heat transfer coefficient for graphene-covered D-SiNWs to the near-field limit is plotted in Figure 4b. With increasing gap distance, the heat transfer coefficient gets closer to the near-field limit. Note that eq 9 is a theoretical limit only for hyperbolic materials rather than a physical upper limit for all materials. Nevertheless, hybrid-

dx.doi.org/10.1021/ph5001633 | ACS Photonics 2014, 1, 785–789

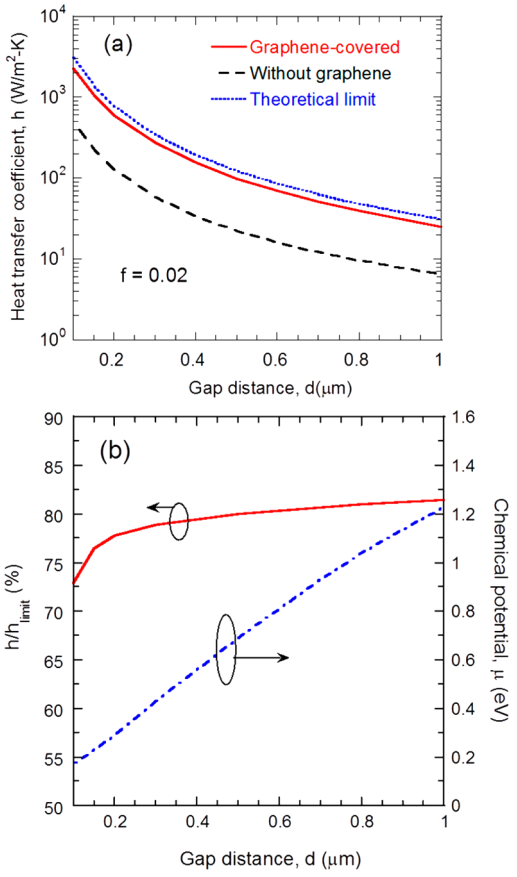

Figure 4. (a) Heat transfer coefficient vs gap distance for D-SiNWs, graphene-covered D-SiNWs with optimal chemical potential, and the theoretical limit given by eq 9 for hyperbolic metamaterials; (b) Ratio of the heat transfer coefficient of graphene-covered D-SiNWs to the theoretical limit as a function of the gap distance. The optimal chemical potential as a function of gap spacing is also shown.

ization of graphene plasmons and hyperbolic modes is demonstrated to achieve a near-perfect photon tunneling and efficient heat transfer that is close to the theoretical limit. From Figure 4b, the optimal chemical potential increases monotonically with d from 100 nm to 1 μm. With decreasing gap distances, the number of contributing modes increases toward high β region in the k-space. In order to postpone the suppression region to larger β, the conductivity of graphene needs to be reduced according to the zero photon tunneling condition. This explains why the chemical potential should decrease with gap spacing.

In conclusion, the near-field blackbody phenomena with perfect photon tunneling having near-unity probability across a broad frequency region and over a large k-space has been theoretically demonstrated based on graphene-covered doped-silicon nanowires. As a result, the near-field radiative heat transfer coefficient achieves as high as 80% of a theoretical limit of hyperbolic materials. The underlying mechanism is due to hybridization of graphene plasmons and hyperbolic modes. This work provides a new way of achieving greatly enhanced photon tunneling and could facilitate a number of relevant applications such as energy harvesting and local thermal management.

AUTHOR INFORMATION

Corresponding Author

*E-mail: zhuomin.zhang@me.gatech.edu.

Author Contributions

†These authors contributed equally to this work (X.L. and R.Z.Z.).

Notes

The authors declare no competing financial interest.

ACKNOWLEDGMENTS

The support from the U.S. Department of Energy, Office of Science, Basic Energy Sciences (DE-FG02-06ER46343) for X.L. and that from the National Science Foundation (CBET-1235975) for R.Z.Z. and Z.Z. are gratefully acknowledged.

REFERENCES

(1) Zhang, Z. M. *Nano/Microscale Heat Transfer*; McGraw-Hill: New York, 2007; pp 425−442.

(2) Guha, B.; Otey, C.; Poitras, C. B.; Fan, S.; Lipson, M. Near-Field Radiative Cooling of Nanostructures. *Nano Lett.* **2012**, *12*, 4546−4550.

(3) Jones, A. C.; Raschke, M. B. Thermal Infrared Near-Field Spectroscopy. *Nano Lett.* **2012**, *12*, 1475−1481.

(4) De Wilde, Y.; Formanek, F.; Carminati, R.; Gralak, B.; Lemoine, P. A.; Joulain, K.; Mulet, J. P.; Chen, Y.; Greffet, J. J. Thermal Radiation Scanning Tunneling Microscopy. *Nature* **2006**, *444*, 740−743.

(5) Otey, C. R.; Lau, W. T.; Fan, S. Thermal Rectification through Vacuum. *Phys. Rev. Lett.* **2010**, *104*, 154301.

(6) Ben-Abdallah, P.; Biehs, S.-A. Near-Field Thermal Transistor. *Phys. Rev. Lett.* **2014**, *112*, 044301.

(7) Park, K.; Basu, S.; King, W. P.; Zhang, Z. M. Performance Analysis of Near-Field Thermophotovoltaic Devices Considering Absorption Distribution. *J. Quant. Spectrosc. Radiat. Transfer* **2008**, *109*, 305−316.

(8) Messina, R.; Ben-Abdallah, P. Graphene-Based Photovoltaic Cells for Near-Field Thermal Energy Conversion. *Sci. Rep* **2013**, *3*, 1083.

(9) Park, K.; Zhang, Z. Fundamentals and Applications of Near-Field Radiative Energy Transfer. *Front. Heat Mass Transfer* **2013**, *4*, 013001.

(10) Shen, S.; Narayanaswamy, A.; Chen, G. Surface Phonon Polaritons Mediated Energy Transfer between Nanoscale Gaps. *Nano Lett.* **2009**, *9*, 2909−2913.

(11) Francoeur, M.; Basu, S.; Petersen, S. J. Electric and Magnetic Surface Polariton Mediated Near-Field Radiative Heat Transfer between Metamaterials Made of Silicon Carbide Particles. *Opt. Express* **2011**, *19*, 18774−18788.

(12) Grigorenko, A. N.; Polini, M.; Novoselov, K. S. Graphene Plasmonics. *Nat. Photonics* **2012**, *6*, 749−758.

(13) van Zwol, P. J.; Thiele, S.; Berger, C.; de Heer, W. A.; Chevrier, J. Nanoscale Radiative Heat Flow Due to Surface Plasmons in Graphene and Doped Silicon. *Phys. Rev. Lett.* **2012**, *109*, 264301.

(14) Lim, M.; Lee, S. S.; Lee, B. J. Near-Field Thermal Radiation between Graphene-Covered Doped Silicon Plates. *Opt. Express* **2013**, *21*, 22173−22185.

(15) Volokitin, A. I.; Persson, B. N. J. Near-Field Radiative Heat Transfer between Closely Spaced Graphene and Amorphous SiO_2. *Phys. Rev. B* **2011**, *83*, 241407(R).

(16) Svetovoy, V. B.; van Zwol, P. J.; Chevrier, J. Plasmon Enhanced Near-Field Radiative Heat Transfer for Graphene Covered Dielectrics. *Phys. Rev. B* **2012**, *85*, 155418.

(17) Ilic, O.; Jablan, M.; Joannopoulos, J. D.; Celanovic, I.; Soljačić, M. Overcoming the Black Body Limit in Plasmonic and Graphene Near-Field Thermophotovoltaic Systems. *Opt. Express* **2012**, *20*, A366−A384.

(18) Liu, X. L.; Zhang, R. Z.; Zhang, Z. M. Near-Field Thermal Radiation between Hyperbolic Metamaterials: Graphite and Carbon Nanotubes. *Appl. Phys. Lett.* **2013**, *103*, 213102.
(19) Biehs, S. A.; Tschikin, M.; Ben-Abdallah, P. Hyperbolic Metamaterials as an Analog of a Blackbody in the Near Field. *Phys. Rev. Lett.* **2012**, *109*, 104301.
(20) Liu, X. L.; Zhang, R. Z.; Zhang, Z. M. Near-Field Radiative Heat Transfer with Doped-Silicon Nanostructured Metamaterials. *Int. J. Heat Mass Transfer* **2014**, *73*, 389−398.
(21) Guo, Y.; Cortes, C. L.; Molesky, S.; Jacob, Z. Broadband Super-Planckian Thermal Emission from Hyperbolic Metamaterials. *Appl. Phys. Lett.* **2012**, *101*, 131106.
(22) Liu, B.; Shen, S. Broadband Near-field Radiative Thermal Emitter/Absorber based on Hyperbolic Metamaterials: Direct Numerical Simulation by the Wiener Chaos Expansion Method. *Phys. Rev. B* **2013**, *87*, 115403.
(23) Fan, G.; Zhu, H.; Wang, K.; Wei, J.; Li, X.; Shu, Q.; Guo, N.; Wu, D. Graphene/Silicon Nanowire Schottky Junction for Enhanced Light Harvesting. *ACS Appl. Mater. Interfaces* **2011**, *3*, 721−725.
(24) Liu, X. L.; Bright, T. J.; Zhang, Z. M. Application Conditions of Effective Medium Theory in Near-Field Radiative Heat Transfer between Multilayered Metamaterials. *J. Heat Transfer* **2014**, *136*, 092703.
(25) Basu, S.; Lee, B. J.; Zhang, Z. M. Infrared Radiative Properties of Heavily Doped Silicon at Room Temperature. *J. Heat Transfer* **2010**, *132*, 023301.
(26) Falkovsky, L. A. Optical Properties of Graphene. *J. Phys. Conf. Ser.* **2008**, *129*, 012004.
(27) Jablan, M.; Buljan, H.; Soljačić, M. Plasmonics in Graphene at Infrared Frequencies. *Phys. Rev. B* **2009**, *80*, 245435.
(28) Biehs, S.-A.; Tschikin, M.; Messina, R.; Ben-Abdallah, P. Super-Planckian Near-Field Thermal Emission with Phonon-Polaritonic Hyperbolic Metamaterials. *Appl. Phys. Lett.* **2013**, *102*, 131106.
(29) Wang, B.; Zhang, X.; Yuan, X.; Teng, J. Optical Coupling of Surface Plasmons between Graphene Sheets. *Appl. Phys. Lett.* **2012**, *100*, 131111.